

Study of band structure in PbSe/PbSrSe quantum wells for midinfrared laser applications

W. Z. Shen, K. Wang, and L. F. Jiang

Laboratory of Condensed Matter Spectroscopy and Opto-Electronic Physics, Department of Physics, Shanghai Jiao Tong University, 1954 Hua Shan Road, Shanghai 200030, People's Republic of China

X. G. Wang and S. C. Shen

National Laboratory for Infrared Physics, Shanghai Institute of Technical Physics, Chinese Academy of Sciences, Shanghai 200083, People's Republic of China

H. Z. Wu and P. J. McCann

School of Electrical and Computer Engineering, Laboratory for Electronic Properties of Materials, University of Oklahoma, Norman, Oklahoma 73019-1023

(Received 30 April 2001; accepted for publication 27 July 2001)

The electronic states in PbSe/Pb_{0.934}Sr_{0.066}Se multiple-quantum-well structures (MQWs) grown by molecular-beam epitaxy have been investigated both theoretically and experimentally for the midinfrared laser applications. With the aid of combined temperature-dependent photoluminescence and absorption measurements on a Pb_{0.934}Sr_{0.066}Se thin film for the effective masses and temperature-dependent band gaps, we find that the PbSe/PbSrSe MQWs have type-I band alignment and the conduction band offset ratio is $Q_c = 0.82 \pm 0.03$. The calculation, taking into account the strain, carrier confinements, and the multivalley band structure, can well explain both the observed luminescence peak energies and the temperature coefficient of the luminescence peaks as a function of well thickness. © 2001 American Institute of Physics. [DOI: 10.1063/1.1406988]

Recently, considerable interest has been devoted to the lead salt IV–VI PbSe-based materials because of their potential opto-electronic applications. The wide tuning range of the energy bands within the ternary Pb_{1-x}Sr_xSe system,^{1,2} the ease in producing good quality material with excellent homogeneity, and the possibility to epitaxial growth on Si substrates,³ have made PbSe and PbSrSe particularly useful for long wavelength infrared intrinsic detectors and midinfrared lasers. The absence of a heavy-hole band reduces the nonradiative Auger recombination rate, one or two orders of magnitude below that of narrow gap III–V and II–VI materials,^{4,5} which is favorable for the reduction of high temperature threshold current. Lower density of states and stronger interband matrix elements allow the appearance of stimulated emission at relatively low generation rates. Strong continuous-wave room temperature stimulated emission luminescence has been observed^{4,5} between 3.0 and 4.0 μm from PbSe/PbSrSe multiple-quantum-well (MQW) laser structures, well above the limit of 2.3 μm in type II quantum cascade laser structures using narrow gap III–V antimonide semiconductor materials.

The motivation of the present study for PbSrSe alloys and their microstructures has been provided by the fact that the fundamental properties, including some important parameters, have been less fully investigated. Lambrecht *et al.*¹ has presented a number of important material parameters for PbSrSe, e.g., the room temperature band gaps, lattice constants, mobilities, and carrier concentrations. However, the temperature-dependent band gaps for PbSrSe, and the strain, band offsets, as well as the subband behavior in a PbSe/PbSrSe MQW system are still lacking. In this letter, we first report combined temperature-dependent photoluminescence (PL) and absorption measurements on a PbSrSe thin film, and then employ successfully the obtained effective masses

and temperature-dependent band gaps of PbSrSe to deduce the band offsets and subband behavior in PbSe/PbSrSe MQW structures with the same Sr composition.

The PbSrSe thin film and PbSe/PbSrSe MQW structures were grown on BaF₂ (111) substrates by molecular-beam epitaxy (MBE) techniques in an Intevac GEN II Modular system. A Sr-to-PbSe flux ratio of 2.9%–3.0% was employed to grow both the PbSrSe thin film and the PbSrSe barriers in PbSe/PbSrSe MQW structures, which yielded Sr composition of around 0.066,^{5,6} also confirmed by x-ray diffraction measurements. The thin film had a layer thickness of around 1 μm , while the 40 periods MQW had the well layer thickness of 40–200 Å, and barrier layer thickness of 400–500 Å. Details of the growth techniques and PL measurements for PbSe/PbSrSe MQW structures have been published elsewhere.^{4,5} The temperature-dependent PL and absorption measurements for the PbSrSe thin film were performed on a Nicolet Nexus 870 Fourier transform infrared spectrometer with an liquid nitrogen cooled InSb detector, a 532 nm laser as the excitation source for PL, and a global infrared source for absorption.

Figure 1 shows the PL and absorption spectra at 10 K for the Pb_{0.934}Sr_{0.066}Se thin film. In the PL spectrum, a single PL peak is observed throughout the temperature range of the measurements (10–300 K). The strong room temperature luminescence observed demonstrates the good quality of the sample. A systematic study⁶ of the dependence of the luminescence spectra on the excitation intensity and temperature reveals four distinct features. At low temperature, the spectra (1) get narrowing, (2) shift the peak to low energy, (3) get increasingly asymmetric with decrease of excitation intensity, and (4) the luminescence intensity increases (unusually) up to the temperature of 100 K and then decreases (as normally expected) with the increasing temperature. Based on

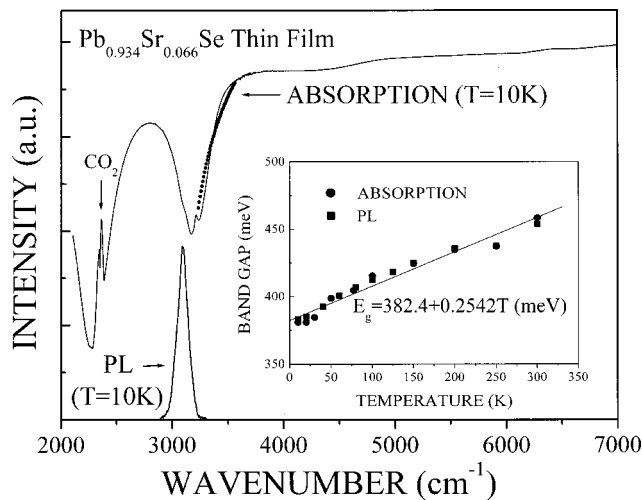


FIG. 1. Experimental photoluminescence (laser excitation intensity of 1.0 W/cm^2) and absorption spectra of a MBE grown $\text{Pb}_{0.934}\text{Sr}_{0.066}\text{Se}$ thin film at 10 K are shown. The solid circles are the theoretical calculation of the absorption edge for effective masses from a six-band $\mathbf{k}\times\mathbf{p}$ model. Shown in the inset is the temperature-dependent band gaps of $\text{Pb}_{0.934}\text{Sr}_{0.066}\text{Se}$ thin film from PL and absorption measurements, together with a linear fit by the solid line.

these, the single luminescence structure has been attributed to localized excitonic line due to the alloy disorder at low temperature, and is gradually delocalized to band-to-band transitions at high temperature.^{6,7} The full width at half maximum (FWHM) is 12.1 meV at 10 K and 67.4 meV at 300 K. In the absorption spectrum, a clear absorption edge is observed, followed by below band gap Fabry-Pérot interference fringes. The absorption edge increases with the temperature, as expected, in the whole measured range. The absorption edge energies are obtained, as widely employed in the literature,^{8,9} from the intersection of the square of the absorption slope with the lowest measured absorption between the interface fringes. A six-band $\mathbf{k}\times\mathbf{p}$ model¹⁰ has been employed to calculate the absorption edge in PbSrSe thin films, shown as solid circles in Fig. 1. The mass anisotropy ratio was estimated from those of the binary alloys (1.8 for PbSe and 3.0 for SrSe) by using linear interpolation scheme. The resultant band gap is in good agreement with this estimation from absorption spectra. From this model, we have also extracted the effective masses for $\text{Pb}_{0.934}\text{Sr}_{0.066}\text{Se}$, which have been used in the subsequent calculation for $\text{PbSe}/\text{Pb}_{0.934}\text{Sr}_{0.066}\text{Se}$ MQW structures. Shown in the inset of Fig. 1 is the band gap energy (E_g) of the PbSrSe thin film, derived both from absorption and PL measurements (via correction due to the band-to-band PL transition above 100 K). It is found that little Burstein-Moss effect is observed in the undoped PbSrSe thin film grown by MBE. The best fit of the experimental results gives $E_g = 382.4 \pm 0.2542 T$ (meV). The derived E_g agrees well with the reported value,¹ and the temperature coefficient dE_g/dT (0.2542 meV/K) decreases with the increase of SrSe content.

The strain of the MQW structures is determined as the relative difference in lattice constants between the PbSe well ($a_{\text{PbSe}} = 6.127 \text{ \AA}$) and $\text{Pb}_{1-x}\text{Sr}_x\text{Se}$ ($a_{\text{PbSrSe}} = 6.137 \text{ \AA}$ for $x = 0.066$) barrier layers, which is approximated as $a_{\text{PbSrSe}} = a_{\text{PbSe}}(1 + 0.025x)$ (\AA).¹ In MQW cases, the PbSe wells will be expected to suffer a tensile strain of 1.65×10^{-3} ,

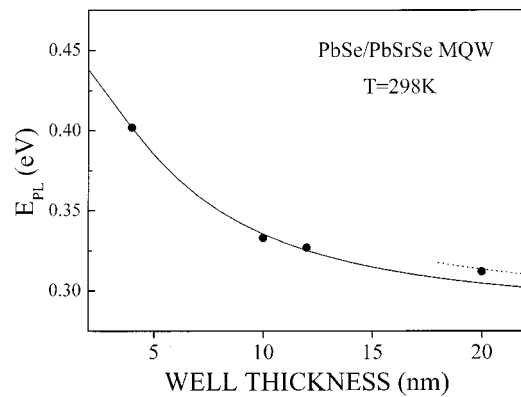


FIG. 2. Theoretical calculation of the luminescence peak energies (E_{PL}) for the (111) valley (solid curve) and $(\bar{1}\bar{1}\bar{1})$ valleys (dotted curve) from $\text{PbSe}/\text{Pb}_{0.934}\text{Sr}_{0.066}\text{Se}$ MQW structures with $Q_c = 0.82$ as a function of well thickness at 298 K is shown. The solid circles are the experimental luminescence peak energies.

while the $\text{Pb}_{1-x}\text{Sr}_x\text{Se}$ barriers can be regarded as unstrained.¹¹ For the (111) growth direction, the strain-induced changes to the PbSe band structure for (111) transverse valley is calculated to be 5.9 meV from the measured elastic constants and from calculated values of the deformation potentials of PbSe .¹² The value is in fair agreement with the experimental relationship between change in strain (0.21%) and change in band gap (6.2 meV) in PbSe .⁹ The substrate-induced strain will not be considered in MQW since there are one 100 nm thick BaF_2 and one very thick ($\sim 3 \mu\text{m}$) PbSrSe buffer layers. The good agreement between theory and experiment shown next reveals that the lattice mismatch is entirely accommodated by strain in well layers without any relief by misfit dislocations present at the heterointerfaces. This also accounts for the strong room temperature luminescence in the MQW structures investigated.

In addition to the strain-induced renormalization of the energy bands, we have also taken into account the electron and hole confinements for MQW structures, which are treated with standard procedures based on an application of the Kronig-Penny model with a parameter of conduction band offset ratio Q_c . Two sets of confinement energy levels, one associated with the (111) transverse valley and the other to the three $(\bar{1}\bar{1}\bar{1})$ oblique valleys, are obtained, and these two sets of energy levels are close to each other for a given quantum number, due to the small ellipsoidal mass anisotropy of PbSe and PbSrSe . The strong luminescence, observed even above room temperature, is consistent with both electrons and holes being confined in the PbSe wells and supports the type-I band alignment for this heterostructure. In the calculation, we have employed the effective masses and bandgaps for PbSe given in Ref. 13, except for $E_g = 0.290 \text{ eV}$ of PbSe at 298 K.¹⁴ The best fit was found to be with the conduction band offset ratio $Q_c = 0.82 \pm 0.03$. Figure 2 displays the calculated luminescence energies at 298 K [solid curve for the (111) valley and dotted curve for $(\bar{1}\bar{1}\bar{1})$ valleys with $Q_c = 0.82$] as a function of well thickness for the $\text{PbSe}/\text{Pb}_{0.934}\text{Sr}_{0.066}\text{Se}$ MQW structures, together with the experimental results⁴ of well thickness of 40, 100, 120, and 200 \AA shown by the solid circles. The measured transition energies for 40, 100, and 120 \AA well structures are in good agreement with the calculation, which confirms the type-I configuration.

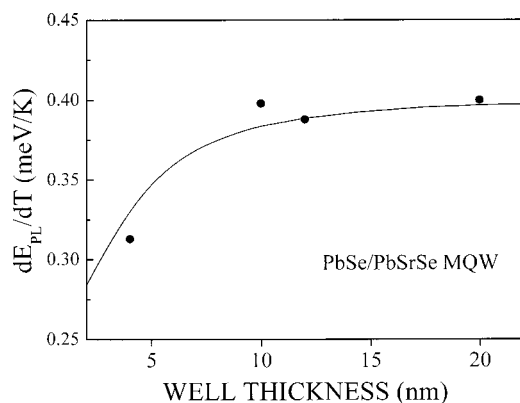


FIG. 3. Temperature coefficient of the luminescence peak energies (dE_{PL}/dT) from PbSe/Pb_{0.934}Sr_{0.066}Se MQW structures as a function of well thickness is shown. Solid curve indicates the theoretical calculation results with $Q_c = 0.82$, solid circles: experimental results.

ration in PbSe/PbSrSe MQW structures (favorable for laser applications).

However, the calculated peak energies in the (111) valley for a 200 Å PbSe well sample are always lower than those of experimental results, no matter what the Q_c is. In this case, the energy levels in the ($\bar{1}\bar{1}\bar{1}$) valleys may also have a contribution to the luminescence structure. The MBE samples were undoped but grown under excess Se flux atmosphere, resulting in being slight *p*-type with carrier concentration of $\sim 1 \times 10^{17} \text{ cm}^{-3}$.¹ The quasi-Fermi energy is estimated to be $E_F = \hbar^2 (3\pi^2 p)^{2/3} / 2m_h = 13.6 \text{ meV}$ (referenced to the valence band edge) with hole effective mass of $0.06 m_0$. Therefore, the lowest hole subband [$E_{lh}^{(\bar{1}\bar{1}\bar{1})} = 11.4 \text{ meV}$] of the ($\bar{1}\bar{1}\bar{1}$) valleys for the 200 Å well structure lies above the quasi-Fermi level, and transitions between ($\bar{1}\bar{1}\bar{1}$) valleys also make a contribution to the luminescence signal. This was not the case for the other three samples. The energy difference (7.7 meV) of the subband energies between the ($\bar{1}\bar{1}\bar{1}$) valleys and (111) valley reasonably accounts for the energy difference ($\sim 6.3 \text{ meV}$) between the theoretical and experimental results shown in Fig. 2 (see the dotted curve).

The aforementioned band structures can explain not only the observed luminescence peaks in PbSe/PbSrSe MQW structures, but also the observed temperature coefficient of the luminescence peaks (dE_{PL}/dT). The calculated luminescence peak energies (in meV) are found to be linear with the temperature, as already demonstrated experimentally.⁴ Figure 3 shows the theoretical calculation results of dE_{PL}/dT as a function of well thickness, together with the experimental results⁴ for the four MQW samples (solid circles). It is clear that the rapid decrease of dE_{PL}/dT at narrow well MQW structures is mainly due to the strong dependence of the subband levels on well width, as a result of small temperature coefficient of the band gaps (dE_g/dT) of the Pb_{0.934}Sr_{0.066}Se barriers. The information for the band structures of the PbSe/PbSrSe MQW can be used to design the double heterostructure lasers. Figure 4 shows the calculated luminescence peak energies as a function of temperature and well thickness [for 20 nm well structure we have used the results for ($\bar{1}\bar{1}\bar{1}$) valleys]. The laser wavelength can be tuned by both the well thickness and the operating temperature. For example, a laser with 12 nm well structure is expected to have a tuning range

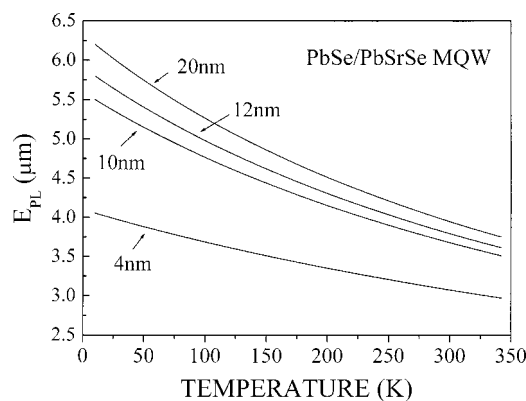


FIG. 4. Calculated luminescence peak energies (E_{PL} in μm , with $Q_c = 0.82$) from PbSe/Pb_{0.934}Sr_{0.066}Se MQW structures as a function of temperature under different well thickness are shown.

from 5.17 to 3.79 μm within temperatures from 77 to 300 K, and have a tuning range from 3.77 to 5.49 μm at 77 K within well thicknesses from 4 to 20 nm.

Finally, we discuss the origin of the luminescence structures in PbSe/PbSrSe MQW structures. The PL intensity was found⁵ to increase with the temperature up to 170–210 K, and then decrease monotonically as the temperature increases, very similar to the case of PbSrSe thin films just mentioned. Therefore, we can attribute to the similar luminescence origin in PbSe/PbSrSe MQW structures to that of the PbSrSe thin films: localized excitonic transition below 170–210 K and band-to-band transitions at a higher temperature. The two-dimensional characteristics in PbSe/PbSrSe MQW structures are evident by the experimental facts of a higher delocalized temperature of 170–210 K and a narrower PL FWHM of $\sim 40 \text{ meV}$ at room temperature, in comparison with 100 K and $\sim 67.4 \text{ meV}$ in PbSrSe thin films.

This work is supported in part by the Natural Science Foundation of China under the contract of 60006005, Shanghai QMX project of 00QA14012, CKSP and TRAPOYT of MOE, P.R.C.

¹A. Lambrecht, N. Herres, B. Spanger, K. Kuhn, H. Böttner, M. Tacke, and J. Evers, *J. Cryst. Growth* **108**, 301 (1991).

²G. Xu, X. M. Fang, P. J. McCann, and Z. Shi, *J. Cryst. Growth* **209**, 763 (2000).

³P. Müller, H. Zogg, A. Fach, J. John, C. Paglino, A. N. Tiwari, M. Krejci, and G. Kostorz, *Phys. Rev. Lett.* **78**, 3007 (1997).

⁴P. J. McCann, K. Namjou, and X. M. Fang, *Appl. Phys. Lett.* **75**, 3608 (1999).

⁵X. M. Fang, K. Mamjou, I. N. Chao, P. J. McCann, N. Dai, and G. Tor, *J. Vac. Sci. Technol. B* **18**, 1720 (2000).

⁶W. Z. Shen, X. G. Wang, Z. G. Qian, L. F. Jiang, S. C. Shen, H. Z. Wu, and P. J. McCann, (unpublished).

⁷F. Fuchs and P. Koidl, *Semicond. Sci. Technol.* **6**, C71 (1991).

⁸P. J. McCann, L. Li, J. E. Furneaux, and R. Wright, *Appl. Phys. Lett.* **66**, 1355 (1995).

⁹H. K. Sacher, I. N. Chao, P. J. McCann, and X. M. Fang, *J. Appl. Phys.* **85**, 7398 (1999).

¹⁰T. R. Globus, B. L. Gel'mont, K. I. Geiman, V. A. Kondrashov, and A. V. Matveenko, *Sov. Phys. JETP* **53**, 1000 (1981).

¹¹W. Z. Shen, S. C. Shen, W. G. Tang, Y. Zhao, and A. Z. Li, *Appl. Phys. Lett.* **67**, 3432 (1995).

¹²S. Rabii, *Phys. Rev.* **167**, 801 (1968).

¹³J. I. Pankove, *Optical Process in Semiconductors* (Dover, New York, 1975), Appendix 2.

¹⁴L. S. Yu, *Semiconductor Heterojunction Physics* (Scientific, Beijing, 1990), p. 14.